Analyzing and modelling functional brain networks

Andrej Jursa, Mária Markošová

Department of Applied Informatics, Faculty of Mathematics, Physics and Informatics
Mlynská dolina, Bratislava
Andrej.Jursa@fmph.uniba.sk, markosova@ii.fmph.uniba.sk

Abstract

Functional brain network is a network extracted from the brain fMRI signal at certain correlation thresholds of the voxel activity. Such network shows, how small brain chunks (voxels) cooperate, even if they are not directly interconnected by axons. These networks are then analysed with a help of standard and also less standard graph theoretical methods, for example graphlet based measures, which are able to compare the graphlet network structures. In agreement with previous studies, our study also shows that the functional brain network degree distribution changes with the correlation threshold. These changes are modelled by a difference equation capturing the processes of node and edge addition. Hill climbing algorithm is then used to optimize model parameters with respect to the data.

1 Introduction

Functional Magnetic Resonance Imaging (fMRI) is a technique for capturing high-resolution images of neural activity in the brain, based on the blood-oxygen-level-dependent (BOLD) signal (Buxton, 2009). FMRI images are captured in a series of three-dimensional slices, with each slice representing a cross section of the brain less than 10 mm thick. A single slice is comprised of a rectangular grid of discrete 3D regions known as voxels (volumetric pixels). Functional brain network captures correlations of voxel signals. Voxel represents a node in the functional brain network. If the absolute value of the correlation coefficient between the two voxel signals crosses certain selected threshold, then there is an edge between these network nodes. Such functional brain network expresses functional cooperation of the brain parts in solving certain cognitive task. If different correlation thresholds are used, one can study, how structural features such as degree distribution and other characteristics evolve due to the changing threshold. Networks investigated in this study are simple and binary undirected graphs. They were extracted by McCarthy (McCarthy et al. 2013, 2014) from the measurements of Buckner et al. (Buckner et al. 2005). In the Buckner's experiment, fMRI brain scans of the three groups of participants - healthy young (HY), healthy elderly (HE), and elderly with Alzheimer (AE), were measured.

Functional brain networks were then analyzed by means of standard statistical and graph theoretical methods (McCarthy et al. 2014).

Here, we also compared pairwise the structure of the functional brain networks using graphlet-based statistical measures (Przulji 2006). This is not common in the functional brain network studies. Graphlet decomposition extends the concept of the node degree distribution. Node degree *k* is a number of edges incident with the node in question and the distribution measures how many network nodes have the degree *k*. From the graphlet point of view, it gives for each *k* a number of nodes touching *k* edges, where an edge is understood as a graphlet G_0. So the degree distribution measures how many nodes touches one G_0, how many nodes touches two G_0 –s…., how many nodes touches k G_0 –s. The same notion can be applied for another 29 (G_1,.., G_{29}) graphlets defined by Przulji (Przulji 2006). However, in the graphlets it is topologically meaningful to distinguish at which automorphism orbit the node touches them. 30 graphlets have 73 different automorfizm orbits, so the correct analogue to the degree distribution is to measure the number of nodes touching particular graphlet at a node belonging to a particular orbit. For example, graphlet G_1 is a chain of three nodes which belong to the two different automorphism orbits (middle node to the one, end nodes to the other). So we ask how many nodes touches one G_1 at the middle node, and how many at the end nodes, how many nodes touches two G_1 –s at the middle and how many at the end nodes, how many nodes touches three G_1-s at the middle and how many at the end nodes …etc. Therefore, we get 73 graphlet degree distributions (GDD). Then one can compare two networks G and H calculating a measure called network GDD agreement either arithmetic $A_{arith}(G,H)$ or geometric $A_{geom}(G,H)$. Both of these measures does not depend on the network parameters, such as number of nodes and edges.

Let $d_G^j(k)$ is a GDD for an orbit j and $S_G^j(k) = d_G^j(k)/k$. The sum of $S_G^j(k)$-s is a norm $T_g^j = \sum_{k=1}^{\infty} S_G^j(k)$. The normalized distribution is calculated

as $N_G^j(k) = S_G^j(k)\ /T_G^j$. Then the distance of the two networks G and H is given as

$$D_G^j(G,H) = \left(\sum_{k=1}^{\infty} \left| N_G^j(k) - N_H^j(k) \right|^2\right)^{1/2} \quad (1)$$

Now the agreement of the two networks is defined as $A^j(G,H) = 1 - D_G^j(G,H)$. Then the arithmetic and geometric agreements are given as arithmetic and geometric averages of particular agreements;

$$A_{arith}(G,H) = \frac{1}{73}\sum_{j=0}^{72} A^j\ (G,H) \quad (2)$$

$$A_{geom}(G,H) = \left(\prod_{j=0}^{72} A^j\ (G,H)\right)^{1/73} \quad (3)$$

The closer these measures are to 1, the more similar is the graphlet structure of G and H network.

Another type of measures we have calculated for the functional brain network are based on the relative graphlet frequency distance (RGFD). We denote $NG_i(G)$ as a number of graphlets of the type $i \in \{1, \dots, 29\}$ in the network G. Then $TG(G) = \sum_{i=1}^{29} NG_i(G)$ is the total number of graphlets in the network G. RGFD is then given as

$$R(G,H) = \sum_{i=1}^{29} |F_i(G) - F_i(H)| \quad (4)$$

where $F_i(G) = -log\left(\frac{NG_i(G)}{TG(G)}\right)$. RGFD is independent of the number of network nodes and edges. Because this measure is from the interval $\langle 0, \infty)$ we used two different yet similar measures proposed by Nehez (Nehez et al 2018), which are both from the interval $\langle 0,1 \rangle$.

To define these measures we define a new $TG'(G) = \sum_{i=0}^{29} NG_i(G)$ in which the zero-th graphlet is added. This will allow to calculate the total variation distance (TVD)

$$\delta(G,H) = \frac{1}{2}\sum_{i=0}^{29} \left| \frac{NG_i(G)}{TG'(G)} - \frac{NG_i(H)}{TG'(H)} \right| \quad (5)$$

The second measure proposed by Nehez (Nehez 2018) is called Hellinger distance, which can be calculated as:

$$HD(G,H) = \left[\frac{1}{2}\sum_{i=0}^{29} \left(\sqrt{NG_i(G)/TG'(G)} - \sqrt{NG_i(H)/TG'(H)}\right)^2\right]^{1/3} \quad (6)$$

In both of these measures holds, the close they are to 0 the more similar is the graphlet structure of G, and H networks.

2 Modelling functional brain networks.

One of our goals is to model by means of difference equations how the functional brain network degree distribution changes with the correlation threshold. The studied networks were acquired at three different correlation thresholds ($\theta_1 = 0.818398$, $\theta_2 = 0.899876$, $\theta_3 = 0.962249$) and further pre-processed by McCarthy and others (McCarthy et al 2014). The threshold choice and other details of data pre-processing are described in (McCarthy et al 2014).

On Fig. 1, the degree distributions derived from the functional brain networks of healthy young participants are depicted. In agreement with other studies (Eguiluz et al. 2005), we found that if the correlation threshold is high, the network has scale-free structure and the power law degree distribution. However, with the decreasing threshold the power law degree distribution is destroyed.

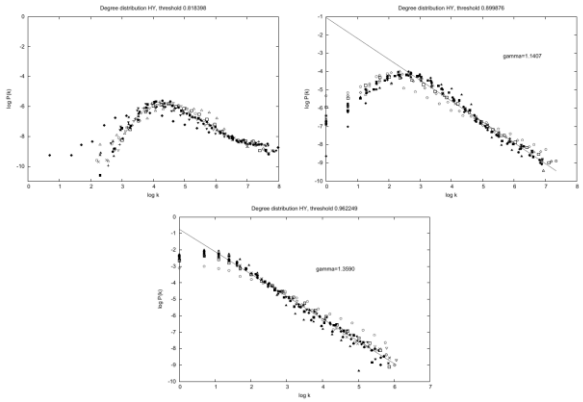

Fig. 1: Degree distributions of the functional brain networks of young healthy participants (HY) from the lowest to the highest correlation threshold. The lowest threshold is 0.818398, the middle one is 0.899876 and the highest is 0.962249. There were 14 participants in this group.

The data for the other groups of participants, namely HE and AE, show the same qualitative picture, although they are less coherent. To imagine, what happen when the threshold decreases, we hypothesise, that the real correlations exhibiting real cooperation of the brain parts create the power law structure. They are more and more disturbed by random correlations as the threshold decreases. In addition, the number of nodes and edges increases, because the lower the correlation threshold is, the more voxel pairs are able to cross it.

In the following analysis, a scenario described in (Scholz et al. 2005) for the noisy scale-free networks inspires us. The authors started from a network with pure scale-free degree distribution. Then, after fixing the number of nodes to N_0 and the initial number of edges to L_0, the network is disturbed by some type of noise: i.e. random link removal, random link exchange and random link addition. The authors have studied how the degree

distribution drifts from the power law character with increasing the noise (randomness) in the network.

We observed the same pattern, namely, that the lowering of the correlation threshold is analogical to increasing the probability of addition of random links in the functional networks, which in turn causes that the degree distribution is not power law any more. In addition, we allow the network to grow, i.e. unlike the original model of Scholz et al. (Scholz et al. 2005), we assume an increase in the number of nodes as the threshold of correlation decreases. We suppose, it is possible to lower the threshold by such a slow way, that at each threshold jump one new node comes to the system. Thus, each step or iteration is marked by addition of a new node. In other words, *n* denotes a number of network growth steps. The rate equation describing the above mentioned dynamic processes in our model is:

$$P(k,n+1) = p_{k,k-1}(n)P(k-1,n) + \left(1 - p_{k+1,k}\right)P(k,n) \quad (7)$$

Here

$$p_{k,k-1}(n) = \frac{a+2b}{N_0+n} + \frac{(a+2b_1)(k-1)}{2L_0+A(n)}, \quad (8)$$

where $A(n) = 2(a+b+a_1+b_1)n$, *P(k,n+1)* is the normalized number of nodes having the degree *k* at the iteration *n+1*. At each iteration, this number changes, due to the fact, that some nodes having at the previous iteration *n* the degree *k-1*, gain a new edge. This is expressed in the first term of the equation (7). The second term expresses, that some nodes have the degree *k* already at iteration *n* and with the probability $1 - p_{k,k-1}(n)$ no new edges are added. In equation (8), N_0, L_0 denote initial number of nodes and edges, *a*, *b* are the number of randomly added edges per iteration, where *a* is the number of edges fetched by a newcoming node and *b* is the number of edges added between older network nodes. Similarly, a_1 denotes the number of edges by which a new node links preferentially to the network and b_1 is the number of edges linking older nodes preferentially. Factor two at some coefficients denotes, that these edges are linked by both of their ends, unlike to those edges, which have one edge end linked to the newcoming node.

To fit the model to the data we used the hill climbing algorithm. Numerical results are presented in the next chapter.

.

4. Results of the numerical simulations

In this section we present results of the numerical simulations. The section is divided into two subsections. In the first one we present the results of the graphlet decomposition of the functional brain networks. The second subsection is devoted to the model (7) numerical simulations and model parameter fitting.

4.1 Graphlet decomposition of the functional brain networks.

We have used ORCA (Hocevar and Demsar 2014) software to compute GDD distribution for functional brain networks of elderly healthy (HE) and elderly Alzheimeric (AE) participants. From these distributions, numbers of particulare graphlet types were derived. Then GDD agreements, together with Hellinger distance and total variation distance have been calculated. Our ambition was to distinguish between the networks of healthy and Alzheimer affected brain networks by means of the graphlet-based statistics. All of these measures compare pairs of networks from the graphlet structure point of view. In our study, we compared each network from the HE group to each network from the AE group.

On Fig. 2, the GDD agreements between functional brain networks of the HE and AE participants are depicted. The minimal agreement is 0.920 and the maximal one is 0.973, which shows a great similarity of the networks between the two groups. This measure is thus not able to distinguish between these two different groups.

Similarly, Fig. 3 shows the total variation and Hellinger distances between functional brain networks of the HE and AE participants. The minimal total variation distance is 0.012 and the maximal one is 0.255. The Hellinger distances are inside the above mentioned interval of the total variation distance. This also shows great similarity of networks from the graphlet structure point of view.

All of these measures have been also calculated between pairs of networks in the same group. The results are similar. That means that the graphlet decomposition methods are in general not too suitable to distinguish between the functional brain networks of healthy and diseased brain. Nevertheless, if we compare the networks of different families, such as random networks and scale free networks all measures show significantly that there is a difference between the graphlet structures of these types of networks.

For example, we compared 9 random graphs with 11 scale-free networks. These data were generated with 500 nodes, having edge probability for random networks between *0.1* to *0.9*. Scale-free networks were generated using configuration model for scaling exponent between *2.5* to *3.5*. The results of similar comparison as mentioned above have the minimal GDD agreement is 0.569 and the maximal one is 0.617. The minimal total variation distance is 0.141 while the maximal one is 0.983. The minimal Hellinger distance is 0.226 and the

maximal is 0.964. The maximal value of both of these measures is one, so they clearly recognize the different structure of the scale free networks and random graphs.

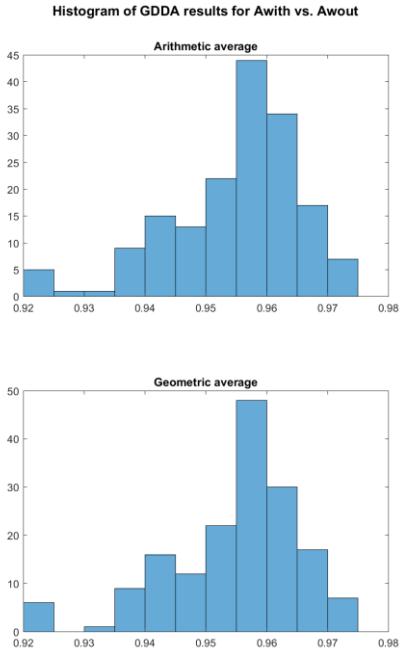

Fig. **2** : Histogram of GDD agreements between functional brain networks of the HE and AE participants. On the x axis there is a GDD agreement, on the y axis the number of network pairs having similar agreements are depicted.

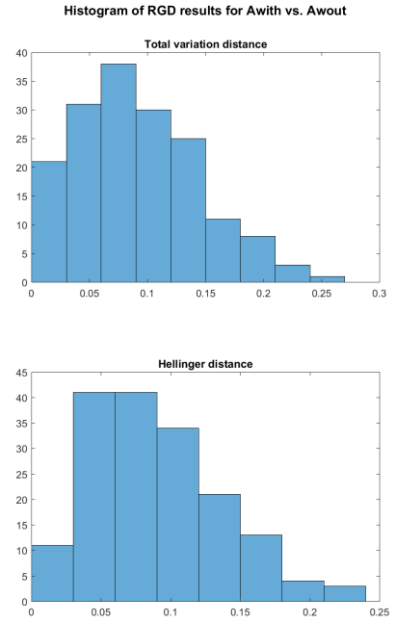

Fig. 3 : Histogram of the total variation and Hellinger distances between functional brain networks of the HE and AE participants. On the x axis there are the distances, on y axis the number of network pairs having similar distances are depicted.

4.2 Numerical simulation of the model

Numerical simulation of the model (7) is done for all functional brain networks from the HY group of participants and compared to the data at the middle correlation threshold θ_2 and the lowest correlation threshold θ_1. Here we present the best fit for the threshold θ_2 together with the best fit for the threshold θ_1 (Fig. 4, Fig. 5).

The simulation is performed as follows. First we used the experimental data to find the parameters in the power law degree distributions at the highest threshold θ_3. This threshold corresponds to the initial number of iterations $n_0 = 0$. As stated before, the initial degree distribution is power-law, i.e.:

$$P(k) = ck^{-\gamma} \qquad (9)$$

Both parameters c and the scaling exponent γ are derived from the data.

In our simulations we first applied the model (7) to model the transition between the two highest correlation thresholds, namely θ_3 and θ_2 of the functional brain networks. The model has been iterated $N_2 - N_0$ times (because at each iteration only one node appears) for the defined set of parameters a, a_1, b, b_1 . N_0, N_2 denote the number of nodes at the initial network state (highest threshold) and at the network state corresponding to the middle correlation threshold, respectively. In each network growth step (a discrete small threshold change) a fixed number of edges is added, namely $(L_2\_L_0)/(N_2 - N_0)$ where L_2 is the number of network edges gained from the measured data at the threshold θ_2 and L_0 is the initial number of edges. To find the best set of parameters a, a_1, b, b_1 we used the hill climbing algorithm, in which the mean square error between the measured and simulated data has been calculated. Each hill climbing simulation have started from seven different initial conditions. From the best fit parameters in the current simulation fifteen new sets of parameters were derived by slight perturbations of the currently best fit parameter set. The hill climbing algorithm has been iterated 800 times. We did the same job as before to model the data at the threshold θ_1. The difference is, that the hill climbing algorithm has been iterated $N_1 - N_0$ times, where N_1 is the number of nodes at the lowest correlation threshold. Also the number of edges added in each threshold (network growth) step is different, namely $(L_1\_L_0)/(N_1 - N_0)$ where L_1 is the number of edges in the functional brain network created at the threshold θ_1. Some results are depicted at Fig.4 and Fig. 5.

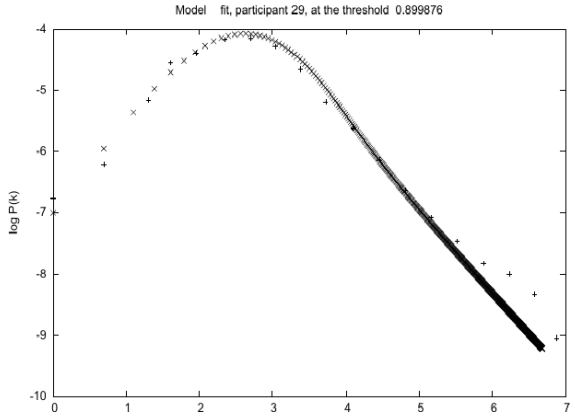

Fig. 4 : The best numerical fit of the model + to the data x at the middle correlation threshold θ_2. Number of iterations is 800. The best fit parameters of the model are $a = 1.3958, b = 3{,}7479, a_1 = 0.0013,$ $b_1 = 243.1351, MSE = 0.2941$

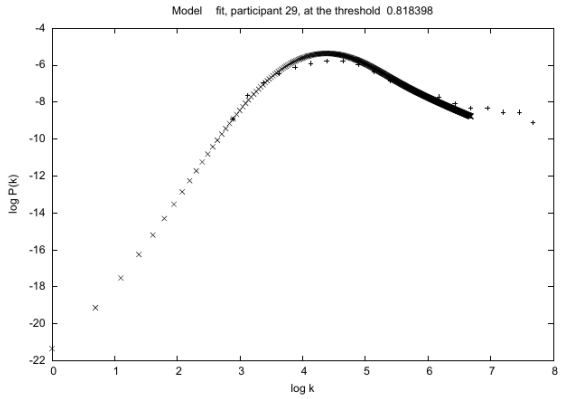

Fig. 5 : The best numerical fit of the model to the data at the lowest correlation threshold θ_1. Number of iterations is 800. The best fit parameters of the model are $a = 4.4472, b = 21.0980, a_1 = 0.0000,\ b_1 = 515.9147, MSE = 0.6877$

We made a similar model fits to all of the networks acquired from the HY group of participants. The MSE of these fits was higher. For the worst fit it was 0.4554 at the threshold θ_2 and 1.184 for the threshold θ_1.

5. Discussion

In this paper, we have shown our studies of the functional brain networks gained from the Buckner et al. (Buckner et al. 2005) experimental measurement of the three groups of participants, namely HY (young healthy), HE (elderly healthy) and AE (elderly with Alzheimer disease) by Paul McCarthy et al. (McCarthy et al. 2013, 2014). McCarthy et al. have studied all of the functional brain networks from the point of view of standard statistical measures, such as clustering coefficient, average shortest path, average degree, etc. Our goal is to apply more sophisticated and not standardly used measures, which compare the topological structure of the pairs of networks, based on the graphlet network decomposition. The other goal is to study the networks degree distributions and their changes with the correlation threshold. Based on these studies, we created a model (7), difference dynamic equation, which includes various processes of node and edge addition. We suppose that these processes occur in the real networks as well.

All three graphlet-based measures, namely the GDD agreement, total variation distance and Hellinger distance show, that they are not able to distinguish between the functional brain networks of Alzheimer affected and healthy brain. We therefore suppose that the graphlet structure is not highly influenced by the Alzheimer brain changes affecting the number of neural connections in the brain. However, from our study it is clear, that the GDD agreement method results have lower variability then the results of the RGFD based methods.

On the other hand, we were able to model qualitatively and quantitatively well the degree distribution changes with the changing correlation threshold in the HY group. We therefore suppose, that the processes captured by our model reflect the real processes. The discrepancies between the model and the real data are because the number of added edges per iteration depends on the threshold. This dependence is more significant the lower the threshold and thus is not a constant as we supposed in the model numerical simulations. How to improve the model and include this fact into it is left for the future studies.

Acknowledgement

We highly acknowledge the support of the VEGA grant number 1/0039/17.

References

Buckner, R. L. (2005). Three principles for cognitive aging research. In R. Cabeza, L. Nyberg, and D. Park (Eds.), *Cognitive Neuroscience of Aging* : 267--285. Oxford University Press.

Buxton, R. B. (2009). Introduction to Functional Magnetic Resonance Imaging: Principles an Techniques (2nd edition). *Cambridge Univ. Press*, Cambridge.

Eguiluz, V. M., Chialvo, D. R., Cecchi, G. A., Baliki, M., Apkarian, A. V. (2005). Scale-free brain functional networks, *Phys. rev. lett*., 94, 018102

Hocevar, T., Demsar, J., A combinatorial approach to

graphlet counting, *Bioinformatics 30*, 4: 559/565

McCarthy, P., Benuskova, L., Franz, E. A. (2013). Functional network analysis of aging and Alzheimer's disease: Results.*Technical Report OUCS-2013-12,* University of Otago, New Zealand.

McCarthy, P., Benuskova, L., Franz, E.A. (2014). The age-related posterior-anterior shift as revealed by voxelwise analysis of functional brain networks. *Frontiers in Aging Neuroscience* 6: 301

Nehez, M. Lelovsky, M. (2018). A Graph Mining Perspective on Graphlet-Based Network Similarity. *In Proceedings of 13th International Workshop on Knowledge Management 2018,* pp. 87-97

Przulji N. (2006), Bio;ogical network comparison using graphlet degree distribution, *Bioinformatics 26*: 177/183

Scholz, J., Dejori, M., Stetter, M., Greiner, M. (2005). Noisy scale-free networks. *Physica A 350*: (2-4), 622--642.